BI-DIMENSIONAL DRIFT CHAMBERS AT FERMILAB

M. ATAC and J. URISH

Fermi National Accelerator Laboratory, Batavia, Illinois, U.S.A.*

Bi-dimensional drift chambers up to 2 m × 1.5 m size using flexible printed circuit balanced delay lines are built. The delay line has good transmission characteristics with 85 Ω impedance and good longitudinal coordinate resolution with geometrical and constructional advantages.

1. Introduction

A large number of secondaries is produced in hadronic collisions at Fermilab and CERN SPS energies. On the average 12 charged particles are produced from a 300 GeV hadron colliding with a stationary target nucleon. Detectors with independent (x,y) coordinate readout of 12 tracks result in very large numbers, of x,y ambiguities. Ambiguous readout becomes an even more complicated problem for colliding beam studies to be conducted at the above-mentioned laboratories. In response to this problem various laboratories have recently developed ways to obtain two correlated coordinates from multiwire proportional chambers or drift chambers[1-7]). The most commonly used bi-dimensional readout methods are charge division and delay-line readout. The results[8]) indicate that the delay line readout produces higher spatial accuracies.

2. Bi-dimensional drift chamber

In this paper we will report the continuing effort on the bi-dimensional drift chamber[3,4]) with flexible printed balanced delay lines which began in 1975 at Fermilab. Since then flat and cylindrical drift chambers using delay lines up to 1.2 m length have been successfully operated by the Experiments 395[9]) and 396[10]) at Fermilab. In this report we will discuss some recent results obtained from a drift chamber using 1.5 m long delay lines. The results have been encouraging enough that two 2 m × 1.5 m (2 m long delay lines) bi-dimensional drift chambers are being constructed for Experiment 400[11]).

Details of the delay line can be found in the previous publications[3,4]), thus they will not be discussed here. A cross-sectional view of the drift cell arrangement is shown in fig. 1. Due to the symmetry and the indicated potentials the electrostatic forces are well balanced. Neither the sense wires nor the delay lines require physical supports when the chamber is held vertically, however, at 40–50 cm intervals pairs of nylon supports are stretched across to improve the rigidity of the delay lines. Each delay line is glued to the nylon wires with a small bead of glue. With this additional support the drift chamber can also be used horizontally. Figs. 2a, 2b and 2c show two end sections and the supported section of a 1.5 m long 3 cell wide model chamber. A magnified section of the delay line in the chamber is shown in fig. 3. The induced pulse is picked up from one of the neighboring sense wires and travels on the printed pattern in two directions towards the ends with a delay rate of 1.85 ns/cm. Thus a 1 cm displacement of track position along the line corresponds to 3.7 ns difference in delay between the ends.

It is sufficient to read the times from two ends of the line to obtain the electron drift time in the gas and the projected position of the track along the delay line.

There is about 20% loss of pulse height per 50 cm in the delay line. Fig. 4 shows this atten-

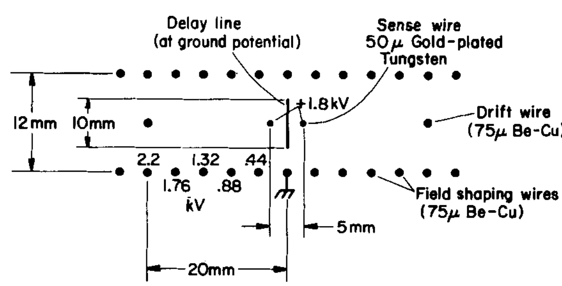

Fig. 1. The cross sectional view of the drift chamber cell.

* Operated by Universities Research Association, Inc., under contract with United States D.O.E.

Fig. 2. (a) End section of the chamber. (b) The other end section of the chamber. (c) The supported section of the chamber.

uation factor as indicated. The line is slightly dispersive for pulses of 10 ns rise time. To obtain the results in these pictures a 50% ethane (C_2H_6) and 50% argon gas mixture was used[4]). Some properties of the gas mixture are indicated in figs. 5 and 6.

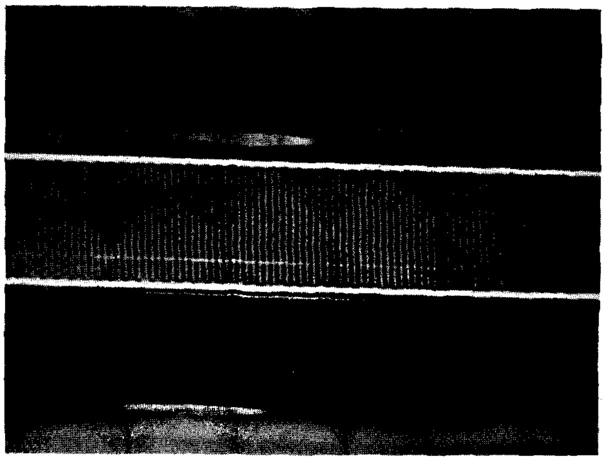

Fig. 3. A magnified section of the delay line.

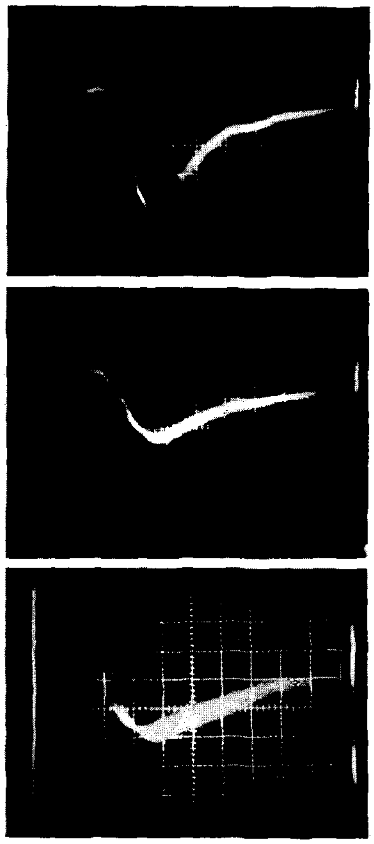

Fig. 4. Pulses obtained from the delay line.

3. Amplifier-discriminator circuit

The delay line amplifier-discriminator circuit is shown in fig. 7. The preamplifier (designed by Boshard, see ref. 3) includes a balanced to unbalanced transformer which produces positive or negative pulses depending on which side of the de-

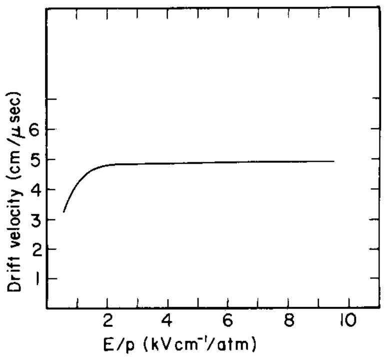

Fig. 5. Drift velocity of electrons in 50% argon–50% ethane gas as a function of E/p.

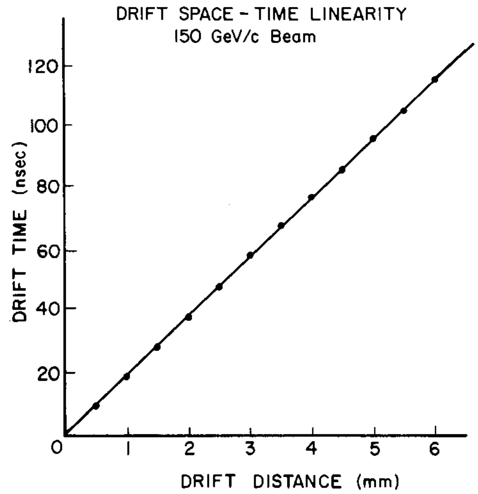

Fig. 6. Drift time to drift distance linearity in the A–C_2H_6 gas mixture.

lay line the induced pulses come from. This eliminates left–right ambiguity for the cell except for the 5 mm region around the sense wires. The input impedance of the amplifier circuit is about 85 Ω which matches with the delay line impedance. Two discriminators are used to detect positive and negative pulses independently. A one-shot is induced to allow adjustable output widths, which are interlocked to prevent overshoot producing an output from the wrong discriminator. At the output a differential transistor pair provides complementary NIM outputs capable of driving 50 Ω cables. These outputs may be easily modified to provide T^2L or ECL outputs.

4. Some results

Some of the characteristics of the chamber were determined from the tests with a collimated ^{55}Fe 5.9 keV X-ray source. The width of the source was approximately 1 mm. A LeCroy QVT 3001 analyzer was used in the T mode to obtain the time difference distribution from the two ends of the delay line. The source was moved in steps of 4 cm from one end to about the midpoint of the line. Fig. 8 shows these distributions. As can be seen in these pictures there is no appreciable dispersive effect. The linearity of the delay line is shown in fig. 9. Spatial resolutions of better than $\sigma = 2$ mm were obtained along the delay line. This would provide a σ of 100 μm from the electron drift time.

The chamber was tested at the M5 test beam of the Meson Laboratory using 40 GeV/c pions. It was moved vertically relative to the beam which was defined by a scintillator telescope. Fig. 10 shows the efficiency distribution obtained from the delay line when pulses from both ends of the delay line were detected. As seen from the figure there is a drop in the efficiency at the nylon support wire. Better than 98% of bi-dimensional efficiency is obtained along the whole cell.

Fig. 11 shows one of the 2 m × 1.5 m bi-dimensional chambers for Experiment 400 in construction. These chambers with hardware processor[12]) will select the angles and consequently the momenta of di-muons which originate from the target.

5. Conclusions

This type of delay line may generally be more practical than other types for the following reasons:

a) Less massive, 75 μm mylar and 25 μm Cu.
b) Flexible and stretchable.
c) Provides good coupling efficiency for induced pulses which is better than 40% of the pulses from the sense wires.
d) Less dispersive than most others.
e) Less noisy, common mode can be easily cancelled out.
f) Commercially available. Buckbee–Mears Co. in St. Paul, Minnesota has produced the delay lines for two other experiments.

The authors would like to express their appreciation to M. Hrycyk and W. Coleman for constructing the chambers.

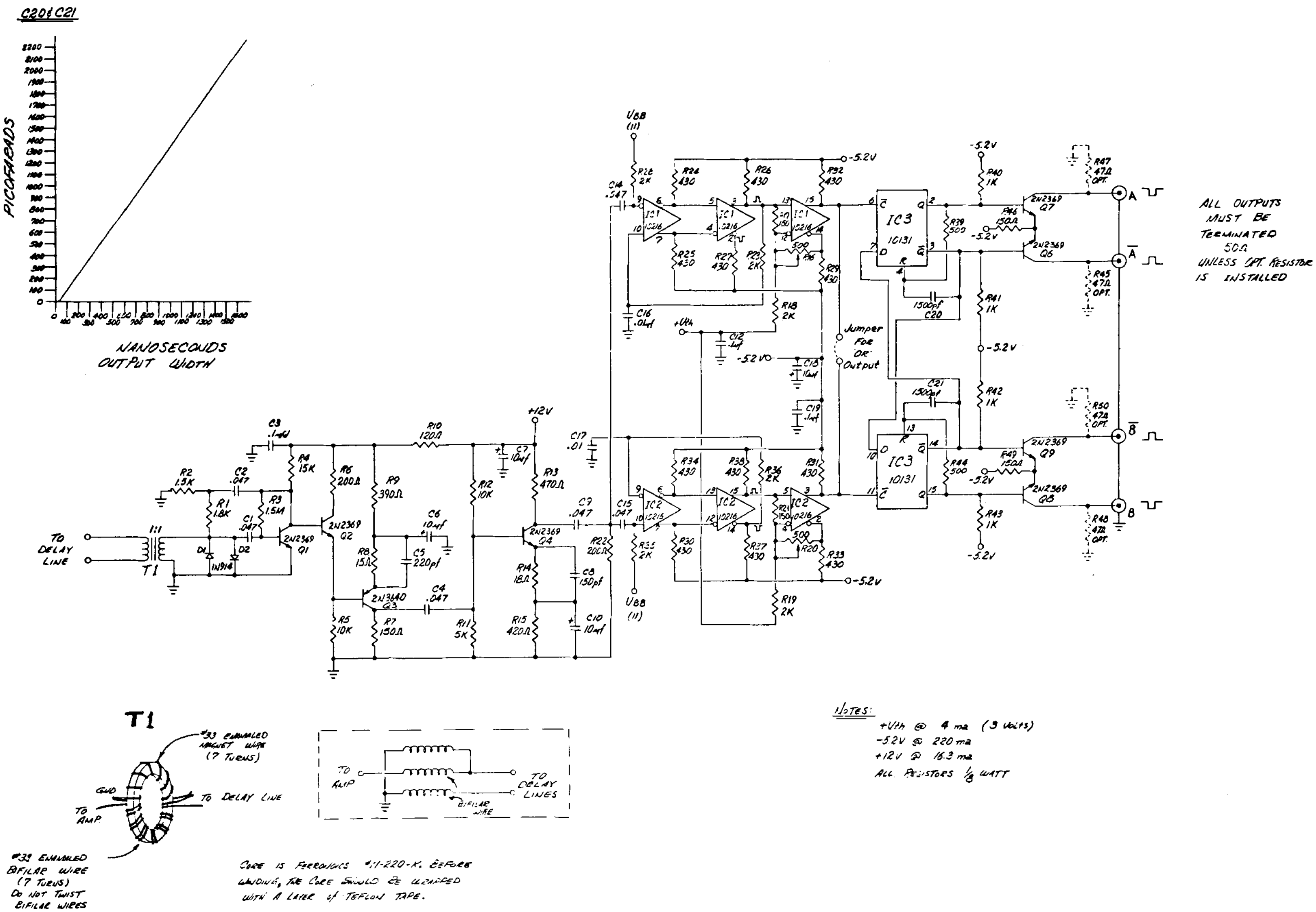

Fig. 7. The amplifier-discriminator circuit.

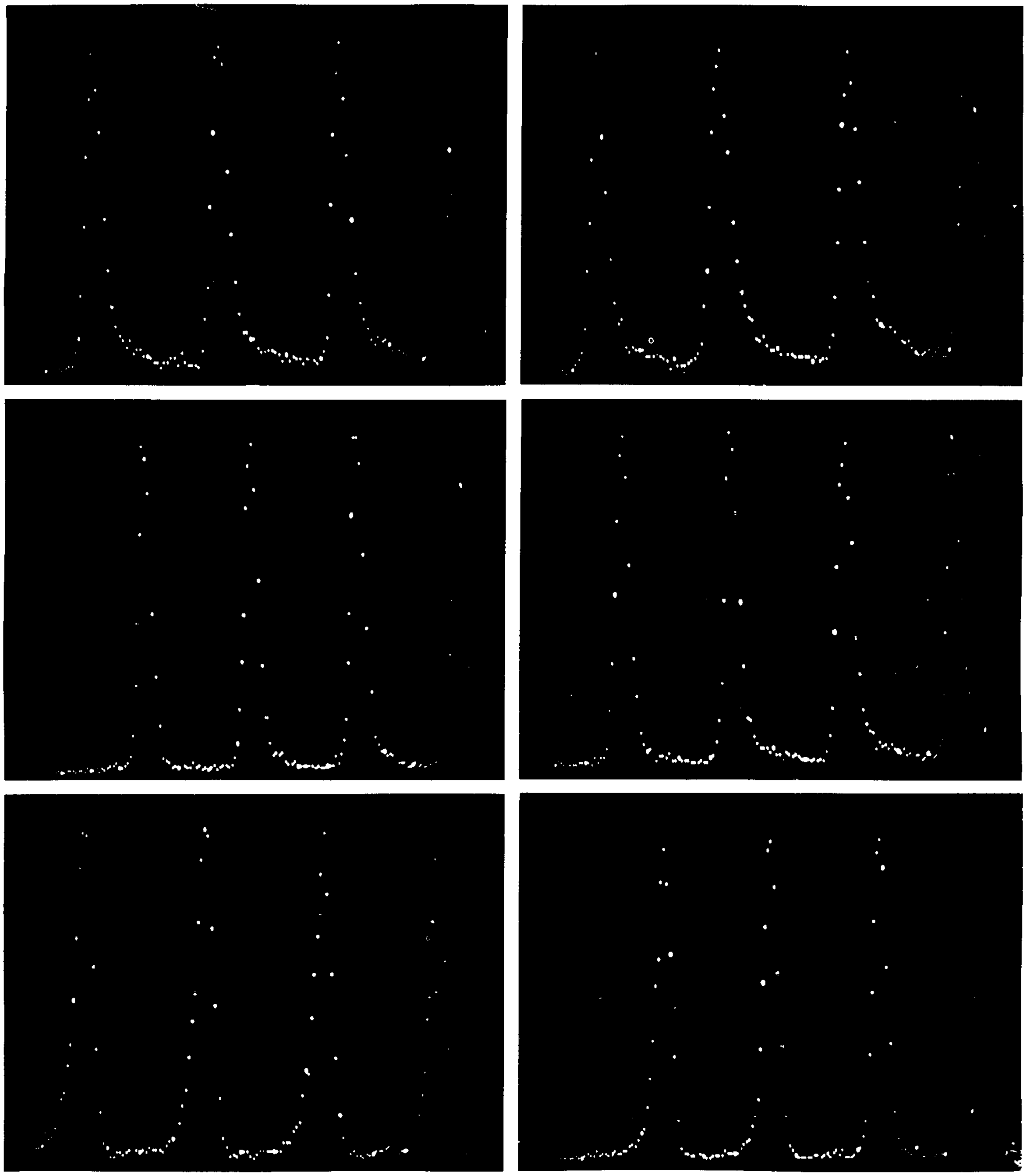

Fig. 8. Difference time distribution along the delay line.

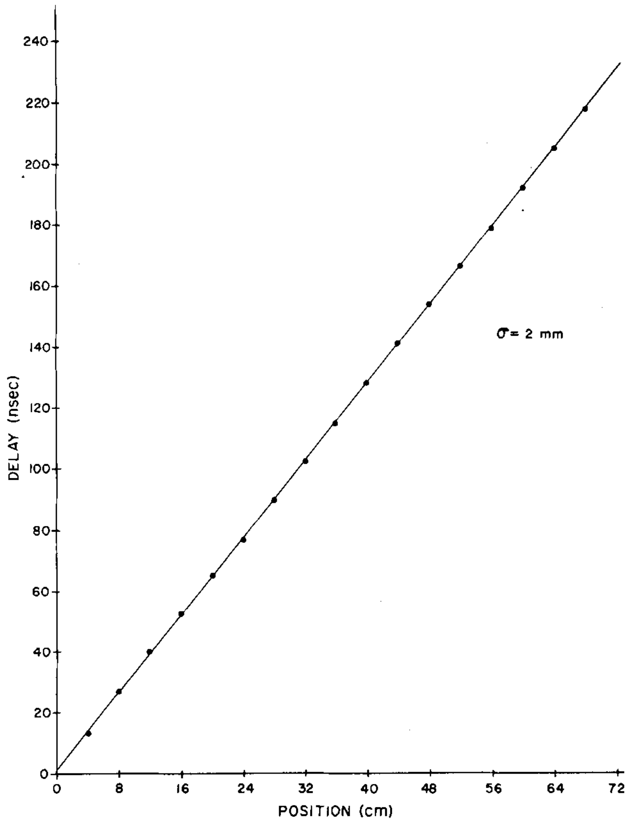

Fig. 9. The linearity of the delay line.

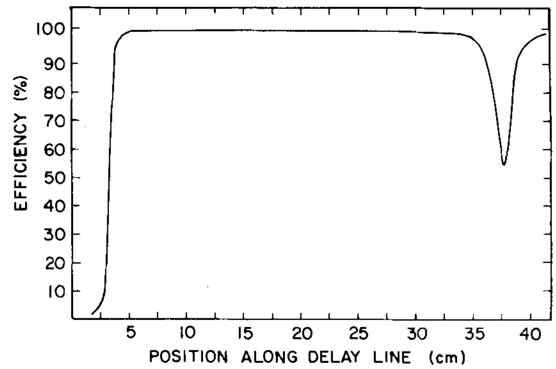

Fig. 10. Efficiency distribution obtained from the delay line.

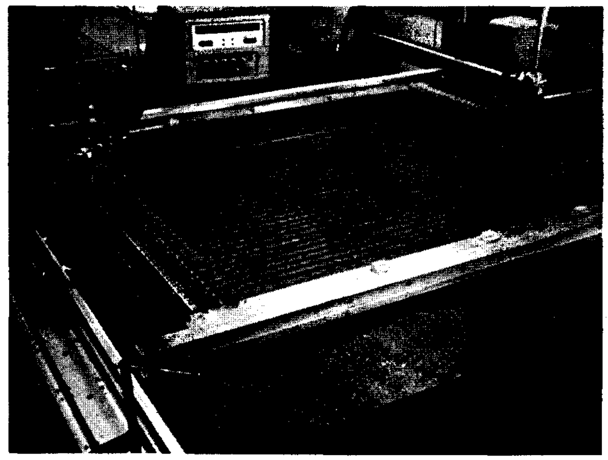

Fig. 11. One of the two 2 m × 1.5 m bi-dimensional drift chambers in construction.

References

1) A. Breskin, G. Charpak, F. Sauli and J. C. Santiard, Nucl. Instr. and Meth. **119** (1974) 1.

2) R. Bosshard, R. L. Chase, J. Fisher and V. Radeka, BNL Report N. 19982, Proc. 2nd ISPRA Symp. on *Nuclear electronics* (1975) EURATOM 5370e, p. 145.

3) M. Atac, R. Bosshard and Y. Kang, Fermilab Internal Report FN-286 (1975).

4) M. Atac, R. Bosshard, S. Erhan and P. Schlein, Nucl. Instr. and Meth. **140** (1977) 461.

5) G. L. Morris, H. A. Thiessen and G. W. Hoffmann, IEEE Trans. Nucl. Sci. **NS-25**, no. 1 (1978).

6) Z. Dimčovski et al., Vienna High Energy Physics Inst. Conf. (1978).

7) O. Achterberg and M. Rössler, Vienna High Energy Physics Inst. Conf. (1978).

8) V. Radeka and P. Rehak, IEEE Trans. Nucl. Sci. **NS-25**, no. 1 (1978).

9) A. Erwin et al., Fermilab Experiment 395.

10) K. Goulianos et al., Fermilab Experiment 396.

11) I. Gaines et al., Fermilab Experiment 400.

12) T. F. Droege, I. Gaines and K. J. Turner, IEEE Trans. Nucl. Sci. **NS-25**, no. 1 (1978).